

# UC Davis

## UC Davis Previously Published Works

### Title

Serum Antibodies to N-Glycolylneuraminic Acid Are Elevated in Duchenne Muscular Dystrophy and Correlate with Increased Disease Pathology in Cmah<sup>-/-</sup>mdx Mice.

### Permalink

<https://escholarship.org/uc/item/5hj6p578>

### Journal

The American journal of pathology, 191(8)

### ISSN

0002-9440

### Authors

Martin, Paul T  
Kawanishi, Kunio  
Ashbrook, Anna  
et al.

### Publication Date

2021-08-01

### DOI

10.1016/j.ajpath.2021.04.015

Peer reviewed



MUSCULOSKELETAL PATHOLOGY

# Serum Antibodies to *N*-Glycolylneuraminic Acid Are Elevated in Duchenne Muscular Dystrophy and Correlate with Increased Disease Pathology in *Cmah*<sup>-/-</sup>*mdx* Mice



Paul T. Martin,<sup>\*†‡</sup> Kunio Kawanishi,<sup>§</sup> Anna Ashbrook,<sup>\*</sup> Bethannie Golden,<sup>¶</sup> Annie Samraj,<sup>§</sup> Kelly E. Crowe,<sup>||</sup> Deborah A. Zygmont,<sup>\*</sup> Jonathan Okerblom,<sup>§</sup> Hai Yu,<sup>\*\*</sup> Agatha Maki,<sup>\*</sup> Sandra Diaz,<sup>§</sup> Xi Chen,<sup>\*\*</sup> Paul M.L. Janssen,<sup>†</sup> and Ajit Varki<sup>§</sup>

From the Center for Gene Therapy,<sup>\*</sup> The Research Institute at Nationwide Children's Hospital, Columbus, Ohio; the Departments of Physiology and Cell Biology,<sup>†</sup> and Pediatrics<sup>‡</sup> and the Graduate Program in Molecular Cellular and Developmental Biology,<sup>||</sup> The Ohio State University, Columbus, Ohio; the Department of Molecular Medicine,<sup>§</sup> University of California, San Diego, California; the Molecular and Human Genetics,<sup>¶</sup> Nationwide Children's Hospital, Columbus, Ohio; and the Department of Chemistry,<sup>\*\*</sup> University of California, Davis, California

Accepted for publication  
April 26, 2021.

Address correspondence to Paul T. Martin, Ph.D., Center for Gene Therapy, The Research Institute at Nationwide Children's Hospital, 700 Children's Dr., Columbus, OH 43205. E-mail: [paul.martin@nationwidechildrens.org](mailto:paul.martin@nationwidechildrens.org).

Humans cannot synthesize the common mammalian sialic acid *N*-glycolylneuraminic acid (Neu5Gc) because of an inactivating deletion in the cytidine-5'-monophospho-(CMP)-*N*-acetylneuraminic acid hydroxylase (*CMAH*) gene responsible for its synthesis. Human Neu5Gc deficiency can lead to development of anti-Neu5Gc serum antibodies, the levels of which can be affected by Neu5Gc-containing diets and by disease. Metabolic incorporation of dietary Neu5Gc into human tissues in the face of circulating antibodies against Neu5Gc-bearing glycans is thought to exacerbate inflammation-driven diseases like cancer and atherosclerosis. Probing of sera with sialoglycan arrays indicated that patients with Duchenne muscular dystrophy (DMD) had a threefold increase in overall anti-Neu5Gc antibody titer compared with age-matched controls. These antibodies recognized a broad spectrum of Neu5Gc-containing glycans. Human-like inactivation of the *Cmah* gene in mice is known to modulate severity in a variety of mouse models of human disease, including the X chromosome-linked muscular dystrophy (*mdx*) model for DMD. *Cmah*<sup>-/-</sup>*mdx* mice can be induced to develop anti-Neu5Gc-glycan antibodies as humans do. The presence of anti-Neu5Gc antibodies, in concert with induced Neu5Gc expression, correlated with increased severity of disease pathology in *Cmah*<sup>-/-</sup>*mdx* mice, including increased muscle fibrosis, expression of inflammatory markers in the heart, and decreased survival. These studies suggest that patients with DMD who harbor anti-Neu5Gc serum antibodies might exacerbate disease severity when they ingest Neu5Gc-rich foods, like red meats. (*Am J Pathol* 2021, 191: 1474–1486; <https://doi.org/10.1016/j.ajpath.2021.04.015>)

Sialic acids (Sias) are negatively charged monosaccharides commonly found on the outer ends of glycan chains on glycoproteins and glycolipids in mammalian cells.<sup>1</sup> Although Sias are necessary for mammalian embryonic development,<sup>1,2</sup> they also have much structural diversity, with *N*-acetylneuraminic acid (Neu5Ac) and *N*-glycolylneuraminic acid (Neu5Gc) comprising the two most abundant Sia forms in most mammalian tissues. Neu5Gc

Supported primarily by NIH grants R01 AR049722 and R01 AR060949 (P.T.M.) and R01 GM32373 (A.V.) and by Japan Society for the Promotion of Science KAKENHI grant JP 19KK0216 (K.K.).

Disclosures: P.T.M. has a financial conflict of interest and receives licensing fees for rAAVrh74.MCK.GALGT2 from Sarepta Therapeutics. P.T.M. is also President and CSO of Genosera Inc.

Current address of K.E.C., Department of Biology, Mount St. Joseph University, Cincinnati, OH; of K.K., Department of Experimental Pathology, Faculty of Medicine, University of Tsukuba, Ibaraki, Japan.

differs from Neu5Ac by having an additional oxygen at the 5-N-acyl position.<sup>3</sup> Neu5Gc synthesis requires the cytidine-5'-monophospho (CMP)-Neu5Ac hydroxylase gene, or *CMAH*, which encodes a hydroxylase that converts CMP-Neu5Ac to CMP-Neu5Gc.<sup>4,5</sup> CMP-Neu5Ac and CMP-Neu5Gc can be utilized by the >20 sialyltransferases to attach Neu5Ac or Neu5Gc, respectively, onto glycoproteins and glycolipids.<sup>1,3</sup>

Humans cannot synthesize Neu5Gc, because of an inactivating deletion in the human *CMAH* gene that occurred approximately 2 to 3 million years ago.<sup>6</sup> This event fundamentally changed the biochemical nature of all human cell membranes, eliminating millions of oxygen atoms on Sias on the glycocalyx of almost every cell type in the body, which instead present as an excess of Neu5Ac. Consistent with the proposed timing of this mutation at around the emergence of the *Homo* lineage, mice with a human-like inactivation of *CMAH* have an enhanced ability for sustained aerobic exercise,<sup>7</sup> which may have provided an evolutionary advantage. In this regard, it is also interesting that the mild phenotype of X chromosome-linked muscular dystrophy (*mdx*) mice with a dystrophin mutation that causes Duchenne muscular dystrophy (DMD) in humans is exacerbated and becomes more human-like on mating into a human-like *CMAH* null state.<sup>8</sup>

Inactivation of *CMAH* in humans also fundamentally changed the immunologic profile of humans. Almost all humans consume Neu5Gc from dietary sources (particularly the red meats beef, pork, and lamb), which can be taken up by cells through a salvage pathway, sometimes allowing for Neu5Gc expression on human cell surfaces.<sup>9-13</sup> Meanwhile, most humans have some level of anti-Neu5Gc-glycan antibodies, defining Neu5Gc-bearing glycans as xeno-autoantigens recognized by the immune system.<sup>13-16</sup> Humans develop antibodies to Neu5Gc not long after weaning, likely triggered by Neu5Gc incorporation into lipo-oligosaccharides of commensal bacteria in the human upper airways.<sup>13</sup> The combination of xeno-autoantigens and such xeno-autoantibodies generates xenosialitis, a process that has been shown to accelerate progression of cancer and atherosclerosis in mice with a human-like *CMAH* deletion in the mouse *Cmah* gene.<sup>17,18</sup> Inactivation of mouse *Cmah* also leads to priming of macrophages and monocytes<sup>19</sup> and enhanced reactivity<sup>20</sup> that can hyperactivate immune responses. *Cmah* deletion in mice also causes hearing loss via increased oxidative stress,<sup>21,22</sup> diabetes in obese mice,<sup>23</sup> relative infertility,<sup>24</sup> delayed wound healing,<sup>21</sup> mitochondrial dysfunction,<sup>22</sup> changed metabolic state,<sup>25</sup> and decreased muscle fatigability.<sup>7</sup>

Given that *Cmah* deletion can hyperactivate cellular immune responses, it is perhaps not surprising that the crossing of *Cmah* deletion in mouse models of various human diseases, to humanize their sialic acid repertoire, can alter pathogenic disease states and disease outcomes. This is true of cancer burden from transplantation of cancer cells into mice,<sup>17</sup> infectious burden of induced bacterial infections in

mice,<sup>13,18,19</sup> and muscle disease burden in response to *Cmah* deletion in the *mdx* model of Duchenne muscular dystrophy<sup>8</sup> and the  $\alpha$  sarcoglycan (*Sgca*) deletion model of limb girdle muscular dystrophy 2D.<sup>26</sup> The *mdx* mice possess a mutation in the dystrophin (*Dmd*) gene that prevents dystrophin protein expression in almost all muscle cells,<sup>27</sup> making it a good genetic model for DMD, which also arises from lack of dystrophin protein expression.<sup>28,29</sup> These *mdx* mice, however, do not display the severe onset of muscle weakness and overall disease severity found in children with DMD, suggesting that additional genetic modifiers are at play to lessen mouse disease severity, some of which have been described.<sup>30-36</sup> *Cmah* deletion worsens muscle inflammation, in particular recruitment of macrophages to muscle with concomitant increases in cytokines known to recruit them, increases complement deposition, increases muscle wasting, and premature death in a fraction of affected *mdx* mice.<sup>8</sup> *Cmah*-deficient *mdx* mice have changed cardiac function.<sup>37</sup> Prior studies<sup>8</sup> show that about half of all mice display induced antibodies to Neu5Gc, which correlates well with the number of animals showing premature death in the 6- to 12-month period. Unpublished subsequent studies suggest that *Cmah*<sup>-/-</sup>*mdx* mice that lack xeno-autoimmunity often have less severe disease, which likely causes selection for more efficient breeders lacking Neu5Gc immunity over time. Current studies were designed to re-introduce Neu5Gc xeno-autoimmunity into serum-naive *Cmah*<sup>-/-</sup>*mdx* mice and describe the impact of xenosialitis on disease pathogenesis.

## Materials and Methods

### Human Serum

Serum was collected from patients and analyzed using a protocol approved by the Institutional Review Board at Nationwide Children's Hospital (IRB13-00190). Anonymized samples were assayed in a blinded manner for binding to a glycan array.

### Mice

Several strains of mice (*Cmah*<sup>-/-</sup>, *Cmah*<sup>-/-</sup>*mdx*, and *CMAH*<sup>LoxP</sup>*Cmah*<sup>-/-</sup>*mdx*) were bred in the C57BL/6J background and housed at the Research Institute at Nationwide Children's Hospital in accordance with the NIH regulations and specifically approved for this study by the Nationwide Children's Hospital Institutional Animal Care and Use Committee. *Cmah*<sup>-/-</sup> mice were previously generated and have the human-like *CMAH* deletion in the *Cmah* mouse gene.<sup>21</sup> Cre-inducible *CMAH*<sup>LoxP</sup> transgenic mice were also made previously.<sup>38</sup> Mice were placed on one of four diets, normal mouse chow containing protein sourced from soy, casein, edible bird's nest (EBN), or porcine submaxillary mucin (PSM); EBN contains 0.25 mg of Neu5Ac per gram of chow, whereas PSM contains 0.25

mg per gram Neu5Gc, about 40 times the sialic acid found in a casein mouse diet (Dyets, Inc., Bethlehem, PA). Dams were fed one of these four defined diet mouse chows during mating and throughout pregnancy until weaning. After weaning, pups were then fed the same chow until the end point (10 months for casein/soy comparison and 6 months for PSM/EBN comparison). For immunization experiments, *Cmah*<sup>-/-</sup>*mdx* and *CMAH*<sup>LoxP</sup>*Cmah*<sup>-/-</sup>*mdx* mice were analyzed at an end point of approximately 11 months of age. *Cmah*<sup>-/-</sup>*mdx* mice breeders for these experiments were confirmed not to have the *Dock2* copy number variant known to affect immune cell phenotypes.<sup>39</sup>

## Histology/Immunostaining

Skeletal muscles were dissected and snap frozen in liquid nitrogen-cooled isopentane. Hearts were dissected, washed in phosphate-buffered saline (PBS), embedded in OCT freezing medium, and frozen in dry ice-cooled isopentane. All tissue was sectioned at 10  $\mu$ m thickness using a cryostat. Sections were stained with hematoxylin and eosin (Sigma, St. Louis, MO) or immunostained with antibody against Neu5Gc (Biolegend, San Diego, CA; 1:500). For anti-Neu5Gc immunostaining, sections were blocked in 0.5% fish gelatin (in PBS) for 1 hour at room temperature, followed by overnight Neu5Gc antibody incubation at 4°C and Cy3-conjugated donkey anti-chicken IgY secondary antibody (Jackson ImmunoResearch Laboratories, Inc., West Grove, PA; 1:500) for 1 hour at room temperature. Immunostaining was visualized on a Zeiss Axiophot epifluorescence microscope (Carl Zeiss, Jena, Germany) using a rhodamine-specific filter, and images were captured using Zeiss AxioVision LE imaging software version 4.1 (Carl Zeiss). In addition, hearts were stained with Fast Green and Sirius Red (Poly Scientific R&D Corp., Bay Shore, NY) following manufacturer's instructions to visualize tissue fibrosis. Sections were visualized on a Zeiss Axioskop 40 microscope (Carl Zeiss) with AxioCamICc3 camera system (Carl Zeiss). Measures of central nuclei, myofiber diameter, and nonmuscle area were done using hematoxylin and eosin-stained sections, as previously described.<sup>8</sup>

For image quantification, investigators were blinded to sample groups until the full analysis was completed. Percentage nonmuscle area was measured for hematoxylin and eosin-stained muscle sections of diaphragm and gastrocnemius, and percentage fibrotic area was measured on Sirius Red- and Fast Green-stained sections of heart, with five samples analyzed per mouse data point. Nonmuscle area was measured by outlining the areas of fibrosis using the freehand tool in ImageJ version v1.53h (NIH, Bethesda, MD; <https://imagej.nih.gov/ij>, last accessed March 23, 2021). The total area of the section was determined, and fibrosis was calculated as a percentage of fibrotic tissue per total area. Fibrosis in the heart was measured on Sirius Red/Fast Green-stained heart muscle cross-sections using previously described color deconvolution methods

using the 2 ImageJ plugin developed by Landini et al.<sup>40,41</sup> The total tissue area was measured, and fibrosis was calculated as percentage of fibrotic tissue per total area.

## Serum Creatine Kinase Assay

Blood was collected from the facial vein and allowed to clot for 1 hour at room temperature. Clotted cells were then centrifuged for 15 minutes at 2000  $\times$  g. Serum was collected and analyzed without freezing. Creatine kinase activity was measured using an enzyme-coupled absorbance assay kit (326-10; SEKISUI Diagnostics, Burlington, MA) following manufacturer's instructions. Absorbance was measured at 340 nm every 30 seconds for 4 minutes at 25°C to calculate enzyme activity. All measurements were done in triplicate.

## Measurement of Mouse Serum Anti-Neu5Gc Antibody Titers

Samples were blinded before analysis. Costar 96-well dishes were coated overnight at 4°C with saturating concentration (2  $\mu$ g/well) of base-treated bovine sialomucin. Other wells were coated with a standard curve of mouse IgG standard solutions of 0, 0.06, 0.125, 0.25, 0.5, 1.0, or 2.0 ng/mL. Bovine sialomucin-coated wells were washed the next day with PBS, after which 20 mmol/L sodium periodate solution (in PBS; pH 6.5) or buffer alone was added for 20 minutes in the dark at 4°C. Sodium periodate is added to oxidize N-glycolyl groups on sialic acids, allowing for side-by-side comparisons of Neu5Gc-containing and Neu5Gc-free wells. After incubation, 20 mmol/L NaBH<sub>4</sub> was added to the sodium periodate-containing wells for 10 minutes. All wells were then washed in a solution containing 100 mmol/L sodium chloride (NaCl) and 50 mmol/L sodium acetate (NaC<sub>2</sub>H<sub>3</sub>O<sub>2</sub>) for 10 minutes at room temperature. Wells were then blocked with PBS with 1% chicken ovalbumin (chick protein lacks Neu5Gc) for 1 hour, after which mouse serum samples, diluted 1:100 in PBS with 1% chicken ovalbumin, were added for 2 hours. After three washes of all wells in PBS with 0.1% Tween 20, 100  $\mu$ L goat anti-mouse IgG conjugated to horseradish peroxidase (Jackson ImmunoResearch, West Grove, PA; 115-035-003; diluted 1:7000 in PBS) was added for 1 hour. After three additional washes in PBS with 0.1% Tween 20, 100  $\mu$ L of o-phenylenediamine hydrochloride substrate (20 mmol/L citrate buffer, pH 5.5, with 10 mg o-phenylenediamine hydrochloride and 40 mL H<sub>2</sub>O<sub>2</sub>) was added for 20 minutes, after which the reaction was quenched by addition of 1.5 mol/L H<sub>2</sub>SO<sub>4</sub>. Absorbance was then read on a SpectraMax M3 microplate reader (Molecular Devices, San Jose, CA, USA) at 490 nm. Positive signals for mouse sera (Neu5Gc<sup>+</sup>-Neu5Gc<sup>-</sup>) were then compared with a standard curve generated for purified mouse IgG from the same plate. As for patient control and control serum samples, we diluted those with PBS (1:100) and added 5 mmol/L methyl- $\alpha$ -Neu5Gc for inhibition, as previously described.<sup>42</sup>

## Cell Culture

C2C12 cells were grown in Dulbecco's modified Eagle's medium containing 20% fetal calf serum, 50 U/mL penicillin, and 50 µg/mL streptomycin. Once confluent, cells were induced to fused into myotubes by placement in Dulbecco's modified Eagle's medium containing 2% horse serum, 50 U/mL penicillin, and 50 µg/mL streptomycin for 6 days. During this time, cells were fed either 10 mmol/L Neu5Ac or 10 mmol/L Neu5Gc to alter sialic acid content in the cells.

## HPLC Analysis of Sialic Acid Forms

Neu5Gc and Neu5Ac content in muscle tissue or muscle cells was analyzed by high-performance liquid chromatography (HPLC) on a LaChrom Elite HPLC (Hitachi, Tokyo, Japan) by tagging sialic acids with the fluorogenic substrate 1,2-diamino-4,5-methylene-dioxybenzene (Sigma) using previously described methods.<sup>43</sup> HPLC runs were performed at 0.9 mL/minute in 85% H<sub>2</sub>O, 7% MeOH, and 8% CH<sub>3</sub>CN. Fluorogenic signals were excited at 373 nm and acquired at 448 nm.

## Measures of Skeletal Muscle—Specific Force and Force Drop during Repeated Eccentric Contractions

A total of 10 mice were used per condition, with 5 females and 5 males assessed per group. Assessment of extensor digitorum longus contractile parameters was done as previously described.<sup>44</sup> Briefly, isolated extensor digitorum longus muscles were tied to a force transducer and linear servomotor. Twitch contractions were elicited at 30°C, and the muscle was stretched to its optimal length, after which one to three tetani of 500-millisecond duration using 1-millisecond pulses at 150 Hz were imposed on the muscle. This was followed by 10 repeated eccentric contractions. For each such contraction, the muscle was tetanized for 700 milliseconds and stretched by 5% of its initial length for a duration of 200 milliseconds. Between each repeat, the muscle was allowed to rest unstimulated for 2 minutes. At completion, muscles were weighed and cross-sectional area was calculated, as described previously.<sup>45</sup>

Assessment of diaphragm muscle strip contractility was done as previously described.<sup>46</sup> Briefly, small linear strips of diaphragm muscle were suspended between a force transducer and stimulator hook in an experimental set-up and superfused with Krebs-Henseleit solution at 37°C. Tetanic force was assessed by tetani at 600-millisecond duration, with frequencies ranging from 20 to 180 Hz with a pulse width of 1 millisecond. At completion, muscles were weighed, and cross-sectional area was calculated as described previously.<sup>46</sup>

## Immunization with Neu5Gc- or Neu5Ac-Containing Immunogen

To induce immunity against Neu5Gc, mice were separated into two groups, either immunized with Neu5Gc-containing

immunogen (chimpanzee red blood cell ghosts (RBG) or Neu5Ac-containing immunogen (human RBG) as a control. Briefly, 2- to 3-month-old mice were immunized with a single 100 µL injection of 2 mg/mL of chimpanzee or 2 mg/mL human RBG solution mixed with an equal volume of Freund complete adjuvant (Thermo Fisher Scientific, Waltham, MA). Two separate booster doses were given 1 week apart using a single 100-µL injection of 2 mg/mL of chimpanzee or 2 mg/mL human RBG solution mixed with an equal volume of Freund incomplete adjuvant (Thermo Fisher Scientific), with immunization being complete at 3 to 4 months of age. Serum was collected 2 weeks, 4 months, and 6 months after the last booster, on which enzyme-linked immunosorbent assay measures of anti-Neu5Gc IgG titers were performed.

## Recombinant Adeno-Associated Virus Production and Purification

Recombinant adeno-associated virus (rAAV) rAAVrh74.CMV.*Cre-GFP* was made, purified, and titered by the Viral Vector Core at Nationwide Children's Hospital using the triple transfection technique in HEK293 cells, with purification by iodixanol gradient and anion-exchange chromatography, as previously described.<sup>47,48</sup>

## Injection of rAAVrh74.CMV.*Cre-GFP* Virus

Intravenous (i.v.) injections via the tail vein and intramuscular (i.m.) injection of the quadriceps, gastrocnemius (Gastroc), and tibialis anterior muscles were given using rAAVrh74.CMV.*Cre-GFP*, an AAV vector, to express *Cre* and in turn induce transgenic expression of the *CMAH* transgene in *CMAH*<sup>LoxP</sup> *Cmah*<sup>-/-</sup> *mdx* mice. Quadriceps, Gastroc, and tibialis anterior muscles on the left side of 4- to 5-month-old adult mice were injected with 5 × 10<sup>11</sup> vector genomes (vg; Gastroc and quadriceps) or 1 × 10<sup>11</sup> vg (tibialis anterior) of rAAVrh74.CMV.*Cre-GFP*. Contralateral muscles (right side) were injected with the same volume of sterile PBS (mock infected). Injections were given using a 0.3-mL insulin syringe, near the midpoint of the belly of the muscle. Tail vein injections were given to 4- to 5-month-old adult mice. Briefly, mice were placed in a restraint that allows tail to be easily accessible, and 5 × 10<sup>12</sup> vg of rAAVrh74.CMV.*Cre-GFP* virus or equivalent volume of sterile PBS (mock infected) was injected. All AAV titers were measured using a supercoiled DNA standard.

## Measurement of Human Serum Anti-Glycan Titers on Sialoglycan Microarray Assays Using Paired Neu5Ac- and Neu5Gc-Terminated Glycans

Anti-Neu5Gc IgG responses were generated as relative fluorescence units. The Neu5Ac- and Neu5Gc-terminated sialoglycan pairs were synthesized, as previously described,<sup>49</sup> and printed on Epoxide slides (Thermo Fisher Scientific, Corning, Pittsburgh, PA) at 100 µmol/L in four replicates each in 300 mmol/L phosphate buffer, pH 8.4. Printed glycan microarray slides were blocked with 0.05



mol/L ethanolamine in 0.1 mol/L Tris-HCl, pH 9.0, washed, and dried. Slides were fitted in a multiwell microarray hybridization cassette (AHC4X8S; ArrayIt, Sunnyvale, CA) to divide into eight subarrays. The subarrays were blocked with 1% ovalbumin in PBS, pH 7.4, at room temperature for 1 hour with gentle shaking (all incubations were performed in a humid chamber). The blocking solution was removed followed by incubation with serum diluted 1:250 in blocking buffer and incubated at room temperature for 2 hours with gentle shaking. The slides were washed and incubated with goat anti-human IgG-Cy3, 1.5 µg/mL, in PBS (Jackson ImmunoResearch, West Grove, PA, USA) at room temperature for 1 hour. The slides were subsequently washed and dried. Microarray slides were scanned using the Genepix 4000B microarray scanner (Molecular Devices Corp., Union City, CA), and data analysis was performed using Genepix Pro 7.0 analysis software (Molecular Devices Corp.).

### Measurement of Relative Gene Expression by Quantitative Real-Time PCR

Total RNA was isolated from frozen blocks of skeletal muscles or heart by use of TRIzol reagent (Invitrogen, Carlsbad, CA). RNA was purified on a silica gel-based membrane-containing column (RNeasy; Qiagen, Germantown, MD). Relative transcription levels were assessed by semiquantitative real-time PCR using the  $2^{-\Delta\Delta C_t}$  method, with 18S rRNA as an internal reference.<sup>50</sup> A high-capacity cDNA archive kit (Applied Biosystems, Foster City, CA) was utilized for the reverse transcription RNA as per the manufacturer’s guidelines. Samples underwent real-time PCR in duplicate using a TaqMan ABI 7500 sequence detection system (Applied Biosystems). Primer/probe sets for 18S ribosomal RNA (assay identifier: Hs99999901\_s1), *Sgca* (mm00486068\_m1), *TNFA* (mm99999068\_m1), *IL1b* (mm00434228\_m1), *Dag1* (mm00802400\_m1), *Ccl5* (mm01302427\_m1), *Ccl3* (mm99999057\_m1), *Ccl2* (mm99999056\_m1), *Col3a1* (mm00802331\_m1), *Colla1* (mm00801666\_g1), *CD68* (mm00839636\_g1), *CD4* (mm00442754\_m1), and *CD8* (mm0011821108\_m1) were purchased from Applied Biosystems (Thermo Fisher Scientific), and primer/probe sets to *Lama2* (mm.PT.58.5945984) and *Lgals3* (mm.PT.58.8335884) were purchased from Integrated DNA Technologies (Coralville, IA).

### Statistical Analysis

Analysis of significance between human serum titer data sets with age was done using linear regression analysis with post-hoc Tukey pairwise comparison. All other comparisons were done using analysis of variance for comparisons of three data sets or more and an unpaired two-tailed *t*-test for comparisons of two data sets. Statistical analysis was done

using GraphPad Prism version 7.0 (GraphPad Software Inc., La Jolla, CA).

## Results

### Increased Serum Anti-Neu5Gc Antibodies in Patients with Duchenne Muscular Dystrophy

The first goal of these studies was to determine whether patients with DMD had anti-Neu5Gc antibodies in their serum and whether these levels were elevated relative to age-matched normal human subjects. This was done by comparing serum antibody binding of 22 DMD and 16 otherwise normal subjects with a sialoglycan microarray presenting glycans terminating in Neu5Gc or Neu5Ac (Figure 1). The average age of DMD subjects studied was 13.3 years, whereas the average age of normal subjects was 11.3 years. The glycan array contained 23 sets of matched Neu5Gc- or Neu5Ac-containing glycans with sialic acid at their terminal end. Five of these matched glycans had multiple sialic acids, where a single Neu5Ac or Neu5Gc was varied. Gal $\alpha$ 1-3Gal $\beta$ 1-4GlcNAc $\beta$ -R was also present on the array as positive control for an  $\alpha$ Gal transplantation antigen (all humans have anti- $\alpha$ Gal antibodies). Neu5Gc-specific titers were calculated by subtracting out Neu5Ac titers for the same glycan from the total Neu5Gc signal (Supplemental Figures S1 and S2), assuming Neu5Ac signals were the result of non-specific antibody binding, as Neu5Ac is expressed in all humans. All signals on the array

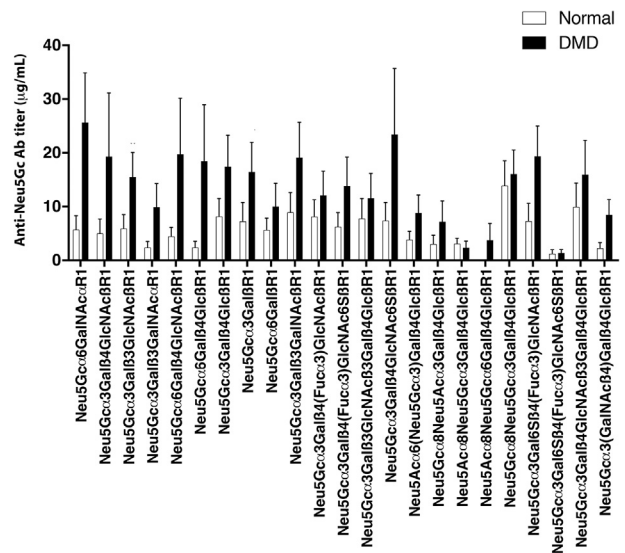


**Figure 1** Serum antibody (Ab) titers to Neu5Gc-containing glycans in otherwise normal subjects and patients with Duchenne muscular dystrophy (DMD). Matched glycans ending in Neu5Gc and Neu5Ac for 23 different glycan structures were spotted on a glycan array and compared for antibody binding from serum samples of patients with DMD (closed bars) and age-matched otherwise normal subjects (open bars). Titers were calculated through comparison with known human IgG standards. Levels from Neu5Ac-containing structures were subtracted from Neu5Gc levels to calculate Neu5Gc-specific antibody titers for each structure. Error bars are SEM. *n* = 22 DMD; *n* = 16 normal.

were compared with a standard curve of human IgG to quantify antibody binding.

Increased average anti-Neu5Gc-specific serum antibody titers for DMD subjects occurred on almost all Neu5Gc-containing structures studied, regardless of  $\alpha$ 2-3,  $\alpha$ 2-6, or  $\alpha$ 2-8 Sia linkage to the underlying glycan (Figure 1). When plotted as individual points instead of as the average value for all samples (Supplemental Figure S3), anti-Neu5Gc-specific titers varied greatly between human samples, >10-fold between individual subjects, which was also true for the  $\alpha$ Gal transplantation antigen. Elevated average DMD titers, however, resulted from elevations in multiple DMD subjects in all instances. The number of individuals with Neu5Gc titers above the mean value, when averaging measures in all 23 Neu5Gc glycans, was  $6.4 \pm 0.4$  of 22 for DMD subjects and  $4.8 \pm 0.2$  of 16 for normal subjects. Although neither of these were the 50% expected for a normal distribution, 29% of DMD subjects and 30% of normal subjects showed titers about the mean. Comparisons of Neu5Gc titers between DMD and normal subjects for individual glycan structures did not significantly differ because of the high variability between samples within each group. Averaging the Neu5Gc-specific titers for all glycan structures where Neu5Gc or Neu5Ac was compared as the terminal glycan indicated an  $3.4 \pm 0.4$ -fold elevation of Neu5Gc titer in DMD relative to normal ( $P < 0.001$ ) controls. In addition, anti-Neu5Gc antibody titers of 11 of the 23 Neu5Gc-containing glycans were significantly ( $P < 0.05$ ) diminished with age in DMD subjects by linear regression analysis, perhaps reflecting the loss of muscle tissue with disease progression (data not shown). A comparison of titers taken from a single DMD subject, spaced 5 months apart, also showed variability in anti-Neu5Gc glycan titer levels for some structures (Supplemental Figure S4), although the overall level of titer elevation among all Neu5Gc-containing glycans was roughly equivalent between the two time points.

A second, less linkage-specific, method was used to measure anti-Neu5Gc antibody titers that involved probing serum with a sialylated glycoprotein to determine whether elevated Neu5Gc titers occurred in other muscle diseases, including Becker muscular dystrophy and inclusion body myositis (Supplemental Figure S5). Titers were again highly variable between subjects, but DMD subjects showed a significant ( $P < 0.05$ ) 5.7-fold increase in titer relative to normal controls, with 7 of 11 DMD samples showing a positive Neu5Gc titer compared with 8 of 32 normal samples. Elevations in Becker muscular dystrophy subjects were less pronounced (a 2.2-fold increase, not significant), whereas inclusion body myositis sera were increased 3.9-fold (not significant) compared with normal controls. These antibody titer studies demonstrate that patients with DMD can have elevated Neu5Gc-specific antibody titers relative to normal subjects, that such antibodies recognize Neu5Gc in the context of multiple subterminal glycans to which it is linked, and that such elevations in Neu5Gc titers may occur in multiple inflammatory muscle diseases.

## Lack of Neu5Gc Antibody Titers or Increased Disease Severity in *Cmah*<sup>-/-</sup>*mdx* Mice Fed Neu5Gc-Rich Diets

Early studies on *Cmah*<sup>-/-</sup>*mdx* mice found increased muscle inflammation, increased muscle wasting, and increased premature death with age relative to that in controls.<sup>8</sup> About half of all mice showed premature death in the 6- to 14-month period. Coincidentally, about half of mice in the same study showed positive titers for Neu5Gc antibodies. Breeding the mice for >15 subsequent generations as homozygotes led to a reduction in the elements of increased disease severity as anti-Neu5Gc serum antibody titers disappeared. Therefore, studies were undertaken to try and recover serum anti-Neu5Gc titers in serum-naïve *Cmah*<sup>-/-</sup>*mdx* mice to address the relationship of such titers to disease severity, beginning with altering dietary Neu5Gc content.

Serum-naïve *Cmah*<sup>-/-</sup>*mdx* mice were fed either casein, a Neu5Gc-containing protein source, or soy, a Neu5Gc-free

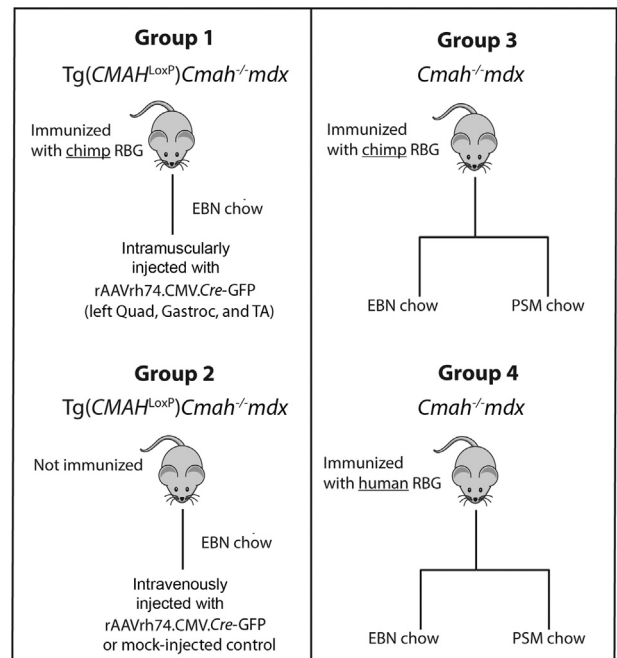


**Figure 2** Experimental plan for studying Neu5Gc immunity and expression. Inducible transgenic (Tg) *CMAH*<sup>LoxP</sup> *Cmah*<sup>-/-</sup>*mdx* mice were used in groups 1 and 2 to allow for *Cre*-mediated induction of *CMAH* transgene expression, whereas *Cmah*<sup>-/-</sup>*mdx* mice with no inducible *CMAH*<sup>LoxP</sup> transgene were used in groups 3 and 4. Groups 1 and 2 were fed mouse chow with protein sourced from edible bird's nest (EBN), which is Neu5Gc free, whereas groups 3 and 4 were fed either EBN chow or chow formulated with porcine submaxillary mucin (PSM), which contains Neu5Gc. Neu5Gc immunity was induced in groups 1 and 3 by immunization with chimpanzee (chimp) red blood cell ghosts (RBGs), which contain Neu5Gc, whereas group 4 was immunized with human RBGs, which do not contain Neu5Gc. Group 2 was not immunized. Neu5Gc expression was stimulated by inducing *CMAH* gene expression in group 1 with i.m. injection of rAAVrh74.CMV.Cre-GFP into the quadriceps (Quad), gastrocnemius (Gastroc), and tibialis anterior (TA) muscle in one leg and in group 2 with i.v. injection of the same vector. For groups 3 and 4, the only source of Neu5Gc expression was dietary Neu5Gc.

protein source, as the protein component of their mouse chow. *Cmah*<sup>-/-mdx</sup> mice fed a casein diet from conception (ie, feeding of pregnant dams) onward until 10 months of age showed only low anti-Neu5Gc staining in skeletal muscles, unlike staining in *Cmah*<sup>+/+</sup> muscle (Supplemental Figure S6). This was coupled with punctate non-specific staining from the secondary antibody, which was a common occurrence. No measurable Neu5Gc serum antibody titers were identified in casein-fed *Cmah*<sup>-/-mdx</sup> mice (data not shown), and no significant changes in muscle tissue pathology or wasting, or in muscle function, occurred when compared with *Cmah*<sup>-/-mdx</sup> mice fed soy chow, including measures of percentage of myofibers with central nuclei (Supplemental Figure S7A), average myofiber diameter (Supplemental Figure S7B), percentage of nonmuscle area (Supplemental Figure S7C), serum creatine kinase activity (Supplemental Figure S7D), and muscle-specific force in the extensor digitorum longus and diaphragm muscle (Supplemental Figure S8, A and B). There were, however, several exceptions; force drop on repeated eccentric contractions in the extensor digitorum longus of *Cmah*<sup>-/-mdx</sup> mice was reduced (Supplemental Figure S8C), total diaphragm force was increased in *mdx* and *Cmah*<sup>-/-mdx</sup> mice fed the soy diet relative to mice fed the casein diet (Supplemental Figure S8B), and there was a significant decrease in nonmuscle area in the gastrocnemius muscle for soy-fed versus casein-fed wild-type mice (Supplemental Figure S7C). In addition, there was a trend toward increased Gastroc muscle wasting (Supplemental Figure S7C), elevated serum creatine kinase (Supplemental Figure S7D), and reduced diaphragm tetanic force (Supplemental Figure S8B) in *Cmah*<sup>-/-mdx</sup> mice relative to *mdx*, regardless of diet.

To further enrich for Neu5Gc in diet, mice were fed a chow formulated with PSM, a protein source that increased

Neu5Gc content 40-fold relative to casein, or EBN, a Neu5Gc-deficient Neu5Ac-rich protein source. Again, PSM-fed mice showed low levels of Neu5Gc immunostaining (Supplemental Figure S9), a pattern consistent with Neu5Gc staining previously reported in normal human and DMD muscle biopsies.<sup>8,51</sup> Neu5Gc expression, however, could not be identified by HPLC analysis (Supplemental Figure S10), suggesting expression could only be observed with the more sensitive immunostaining method. C2C12 myotube cultures, which can take up Gc-containing monosaccharides,<sup>52</sup> were used herein as a positive control. Thus, even over the course of months, dietary uptake of sialic acid, in a protein source, provided for only minor incorporation of Neu5Gc content to skeletal myofibers of *Cmah*<sup>-/-mdx</sup> mice, with no induction of anti-Neu5Gc antibodies or worsening of disease phenotypes.

### More Severe Disease Phenotypes in *Cmah*<sup>-/-mdx</sup> Mice with Neu5Gc Expression and Anti-Neu5Gc Antibodies

To address the role of Neu5Gc immunity, a four-cohort study was undertaken with both Neu5Gc expression, either through diet or *CMAH* transgene expression, and immunization with Neu5Gc as variables (Figure 2). In groups 1 and 2, LoxP-flanked *CMAH* transgenic *Cmah*<sup>-/-mdx</sup> mice (*CMAH*<sup>LoxP</sup>*Cmah*<sup>-/-mdx</sup>) were used to allow for induction of *CMAH* gene expression by Cre-mediated recombination. Cre expression was induced by injection of an AAV vector bearing the *Cre* transgene as a fusion protein with green fluorescent protein (GFP; rAAVrh74.CMV.*Cre*-GFP), as done previously.<sup>53</sup> *CMAH* transgene expression was induced either in the muscles of a single limb (group 1), by i.m. injection, or systemically in all muscles and nonmuscle tissues (group 2) by i.v. injection. Group 1 and 2 mice were fed EBN chow so as to eliminate possible dietary Neu5Gc loading.

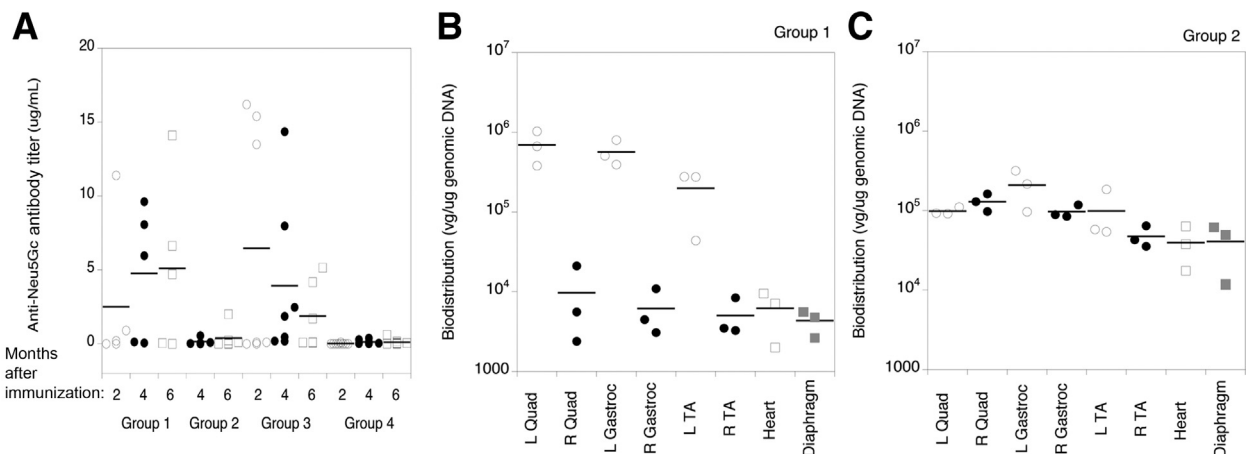


**Figure 3** Serum antibody titers to Neu5Gc and biodistribution of adeno-associated virus (AAV) vectors. **A:** Anti-Neu5Gc antibody titers were measured in serum in all mice in groups 1 to 4 at 2 weeks (open circles), 4 months (closed circles), and 6 months (open squares) after the final immunization. **B** and **C:** AAV vector genome (vg) biodistribution was quantified in group 1 (**B**) or group 2 (**C**) muscles, including left (L; open circles) or right (R; closed circles) quadriceps (Quad), gastrocnemius (Gastroc), and tibialis anterior (TA), as well as heart (open squares) or diaphragm (gray squares). Lines show the mean value for each group. AAV vg were measured relative to 1  $\mu$ g of genomic DNA.  $n = 5$  to 9 per group (**A**);  $n = 3$  per group (**B** and **C**).



Groups 3 and 4 consisted of *Cmah*<sup>-/-</sup>mdx mice with no floxed *CMAH* transgene. Herein, mice were fed either PSM or EBN chow to allow for comparison of Neu5Gc provided from diet (with PSM having Neu5Gc and EBN not). Group 3 (and group 1) had serum anti-Neu5Gc antibodies induced by immunization with chimpanzee RBGs, which are rich in Neu5Gc, whereas group 4 was immunized with human RBGs, which lack Neu5Gc. Mice were given three immunizations, each spaced 1 week apart, between 2 and 4 months of age. AAV-Cre injections were then given to induce Neu5Gc expression (groups 1 and 2) between 4 and 5 months of age, with analysis of tissues done at 6 months after injection (by 11 months of age).

At 2 weeks, 4 months, and 6 months after injection, serum from all four groups was assayed for anti-Neu5Gc antibody titers (Figure 3A). Mice in group 1 had high serum anti-Neu5Gc titers, averaging 4 to 5 µg/mL at 4 and 6 months after immunization. However, development of antibody titers was highly variable between mice, with only three of five mice with titers of ≥4 µg/L at these time points. By contrast, only one mouse in group 2 (of six) had a high titer (2 µg/mL) at 6 months after AAV delivery, whereas several others had much lower, but still measurable, titers (between 0.1 and 0.4 µg/mL). As in group 1, about half of mice in group 3 had high Neu5Gc titers, with the overall average for this group being >6 µg/mL at 2 weeks after immunization. Unlike group 1, however, mice in group 3 showed reduced Neu5Gc titers over time, averaging about 4 µg/mL at 4 months and 2 µg/mL at 6 months. As expected, group 4 showed low anti-Neu5Gc titers (all <0.16 µg/mL at 6 months), as these mice were not immunized with a Neu5Gc-containing antigen. Both group 1 and group 3 showed significant differences ( $P < 0.05$ ) compared with group 4 in Neu5Gc titer, even at 2 weeks after the final immunization.

Measures of AAV biodistribution were sampled in mice in groups 1 to 4 by quantitative PCR against a known DNA standard. Mice with high and low anti-Neu5Gc titers showed similar distributions (data not shown). In group 1, i.m. injections of (left) Gastroc, quadriceps, and tibialis anterior muscles led to transduction with AAV vg levels that exceeded 1 vg per muscle nucleus (or  $1.7 \times 10^5$  vg/µg genomic DNA) (Figure 3B), in theory a saturating level of AAV transduction. On the other hand, systemic i.v. injections in group 2 led to even, but typically subsaturating, levels of AAV in limb muscles. Group 2, however, showed higher transduction in heart and diaphragm than group 1, as expected (Figure 3C). Because the rAAVrh74 serotype is particularly adept at crossing the vascular barrier, some bleed through to noninjected muscles was expected in group 1, although these levels were typically two logarithms below the level of AAV transduction level found in the injected muscles. As expected, group 3 and 4 had undetectable (<50 vg/µg genomic DNA) levels of AAV.

Anti-Neu5Gc immunostaining identified Neu5Gc expression in AAV-Cre-injected muscles in group 1 mice

(eg, in an injected Gastroc) (Figure 4). This local induction of muscle *CMAH* expression, however, resulted in additional Neu5Gc expression in all contralateral noninjected muscles, heart, and diaphragm by 6 months after injection (Figure 4). Although i.m.-injected muscles showed high transduction of the AAV vector, at or exceeding 1 vg/nucleus in muscle tissue, AAV transduction in contralateral noninjected leg muscles, diaphragm, and heart was only 1 vg per 200 nuclei (Figure 3B), which would likely not allow for sufficient *CMAH* transgene expression to see such widespread Neu5Gc staining. Thus, i.m. injection likely resulted in secretion of Neu5Gc-containing glycoproteins from the injected group 1 muscles or from liver (which can take up AAV at high levels, even when muscle is targeted<sup>54</sup>). Similar expression results were obtained after i.v. delivery of *Cre* in *CMAH*<sup>LoxP</sup>*Cmah*<sup>-/-</sup>mdx mice, where at 6 months all muscles showed Neu5Gc expression, whereas mock-injected controls did not (Figure 4). Groups 3

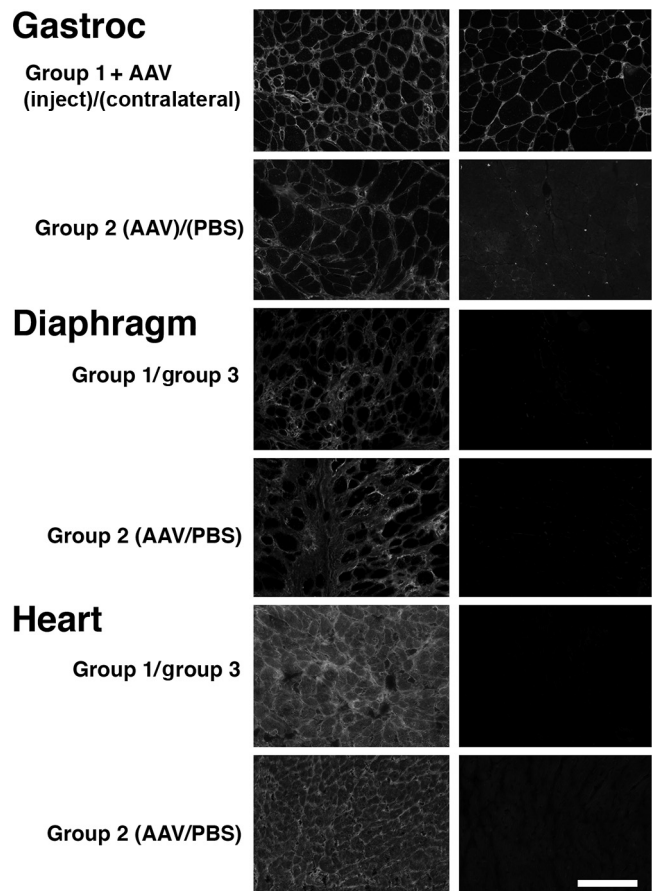


**Figure 4** Neu5Gc immunostaining in skeletal muscle, diaphragm, and heart. Sections from gastrocnemius (Gastroc), diaphragm, and heart muscle were stained with anti-Neu5Gc antibody. Gastroc: Left [group 1; adeno-associated virus (AAV)-*Cre* injected] versus right (group 1; contralateral muscle, mock infected) and left (group 2; AAV-*Cre* injected) versus right [group 2; phosphate-buffered saline (PBS) injected]. Diaphragm and heart: Left (group 1) versus right (group 3) and left (group 2; AAV-*Cre* injected) versus right (group 2; PBS injected). All images shown are time-matched exposures. Scale bar = 200 µm.

(Figure 4) and 4 (data not shown) showed no significant Neu5Gc expression in time-matched images and appeared similar to control (PBS-injected group 2) muscles, suggesting that functional *CMAH* expression was required to achieve high levels of muscle Neu5Gc staining.

There were three significant findings from this experiment. The first was that induction of *CMAH* expression, with concomitant induction of anti-Neu5Gc antibodies, in group 1, led to decreased survival within the 6 months of *Cre*-mediated *CMAH* expression analyzed (Figure 5A). More than half of group 1 mice failed to survive in the 11-month completion age of the experiment, and all group 1 mice that failed to survive died after completion of the immunization and AAV injection. No mice, by contrast, died prematurely in groups 2, 3, or 4. Thus, induction of *CMAH* expression, in the presence of Neu5Gc immunity, led to a shortened lifespan in half of group 1 animals.

The second finding was that the mice that remained in group 1 showed significant increases in muscle wasting, or absence of muscle tissue in muscles sections, relative to control, for both the gastrocnemius and diaphragm muscle (Figure 5, B and C). Group 1 also showed a significant increase in muscle fibrosis in the heart, relative to controls, and to group 3 and group 4 (Figure 5D). Hematoxylin and eosin staining showed increased muscle wasting, which included fat and extracellular matrix deposition, in group 1 relative to group 3, and increased Sirius Red staining in the heart (Figure 6). Interestingly, both group 3 and group 4 also showed a significant increase in muscle wasting in the gastrocnemius relative to controls, which may reflect a role for immunization in exacerbating disease pathology that is independent of Neu5Gc (Figure 5B). This was not the case, however, in the heart (Figure 5D), where group 1 showed a significant increase in fibrosis relative to group 3 or group 4 as well as to control. Group 2 muscles also showed

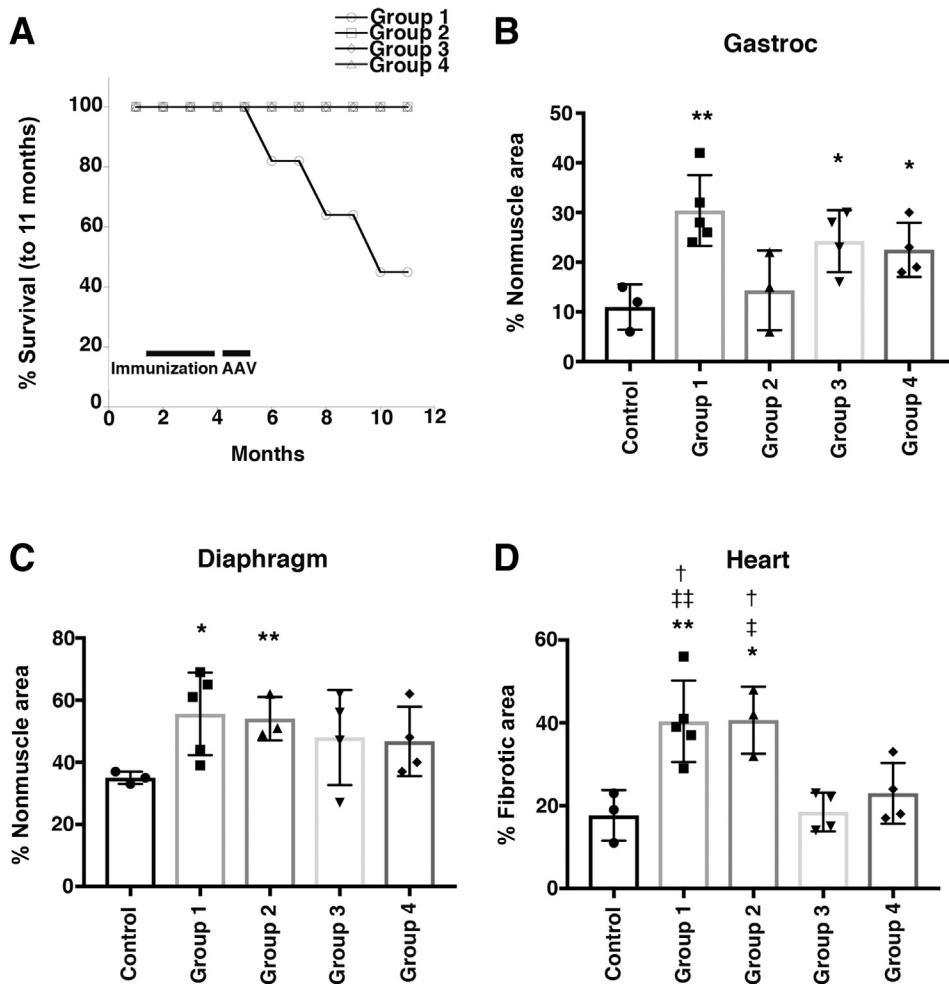


**Figure 5** Decreased survival and increased fibrosis in group 1 mice. **A:** Percentage survival over time up to 11 months was measured in groups 1, 2, 3, and 4. Mice were immunized between months 2 to 4 and injected with adeno-associated virus (AAV) in group 1 between months 4 and 5. **B:** Percentage nonmuscle area was calculated for gastrocnemius (Gastroc) using muscle cross-sections stained with hematoxylin and eosin. **C:** Percentage nonmuscle area was calculated for diaphragm using muscle cross-sections stained with hematoxylin and eosin. **D:** Percentage fibrosis based calculated using Sirius Red/Fast green costaining of heart sections. Error bars are SD (**B–D**).  $n = 3$  to 5 mice per group, with five sections analyzed and averaged per data point. \* $P < 0.05$ , \*\* $P < 0.01$ , any group versus control; † $P < 0.05$ , any group versus group 4; ‡ $P < 0.05$ , †† $P < 0.01$ , any group versus group 3. Gastroc, gastrocnemius.

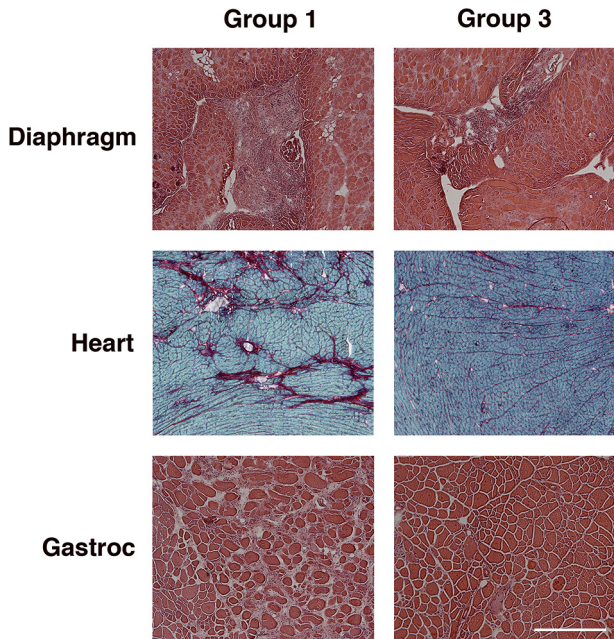


**Figure 6** Evidence of increased fibrosis in group 1 and group 3 muscles. Cross-sections of rolled diaphragm muscle or cross-sections of mounted gastrocnemius (Gastroc) muscle were stained with hematoxylin and eosin, whereas heart sections were stained with Sirius Red and Fast Green. Sections from group 1 and group 3 muscles were compared. Scale bar = 200  $\mu$ m.

significant increases in wasting relative to controls in the diaphragm and increased Sirius Red staining relative to control, group 3, and group 4 in the heart (Figure 5, C and D, and Supplemental Figure S11).

The third finding was that Neu5Gc immunization and/or *CMAH* transgene-induced Neu5Gc expression often correlated with increased gene expression for markers of muscle

inflammation and fibrosis (Figure 7 and Supplemental Figure S12). Group 1 and group 3 both showed significant increases in expression markers of cytotoxic T cells (*CD8*), helper T cells (*CD4*), and macrophages (*CD68*) in the diaphragm, whereas group 1, but not group 3, showed significant increases for these same markers in heart and Gastroc muscles (Figure 7A). Similarly, both groups 1 and 3 showed significant increases in expression for cytokines (*Ccl2*, *Ccl3*, *Ccl5*, *Il1b*, and *Tnf $\alpha$* ) in the diaphragm, whereas again group 1, but not group 3, showed significant increases in the heart and Gastroc (Figure 7B). In addition, group 1 AAV-*Cre*-injected limb muscles showed significant increases for *CD8*, *Ccl3*, *Il1b*, and *Tnf $\alpha$*  expression relative to contralateral (mock-injected) group 1 muscles in the same mice (Supplemental Figure S13). Lastly, both group 1 and group 3 mice showed significant elevations in markers for muscle fibrosis [galectin 3, collagen 1( $\alpha$ 1), and collagen 3( $\alpha$ 1)] relative to mock-injected control in the diaphragm, whereas elevated expression was more variable in heart and Gastroc (Figure 7C).

A comparison of group 3 and group 4 muscles for the same gene expression markers suggested that immunization with Neu5Gc did not lead to significant elevations relative to mice immunized with Neu5Ac (Supplemental Figure S12). By contrast, *Cre*-injected group 2 mice had a significant elevation in *CD8* expression in all three muscles relative to control (Supplemental Figure S12A) as well as significant elevations in most cytokines in diaphragm and heart (Supplemental Figure S12B) and in one heart fibrosis marker, *Colla1* (Supplemental Figure 12C). Hearts in group 2 also showed a significant increase in *Colla1* expression, consistent with increased fibrosis. Expression of three control genes encoding proteins in the muscle sarcolemma,

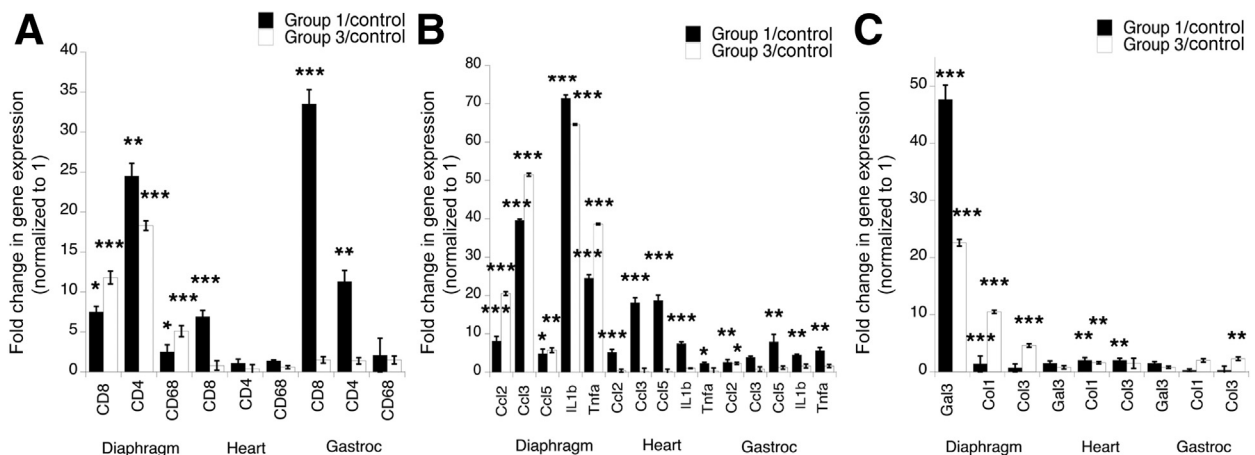


**Figure 7** Relative expression of genetic markers for T cells, macrophages, muscle inflammation, and muscle fibrosis after induction of Neu5Gc immunity with or without *CMAH* transgene expression. Relative gene expression was measured for markers of helper (CD4) and cytotoxic (CD8) T cells and macrophages (CD68; A), muscle inflammatory markers (B), and muscle fibrosis markers (C). Group 1 (closed bars) and group 3 (open bars) were compared with phosphate-buffered saline-injected controls with no Neu5Gc immunity or expression. Error bars are SEM (A–C).  $n = 5$  to 8 mice per group (A–C). \* $P < 0.05$ , \*\* $P < 0.01$ , and \*\*\* $P < 0.001$  for group 1 or group 3 versus control. *Ccl2*, C-C motif chemokine ligand 2 (also monocyte chemoattractant protein 1 or MCP1); *Ccl3*, C-C motif chemokine ligand 3 (also macrophage inflammatory protein 1a or MIP1a); *Ccl5*, C-C motif chemokine ligand 5 (also RANTES or regulated on activation, normal T-cell expressed and secreted); Col1, collagen 1( $\alpha$ 1); Col3, collagen 3 ( $\alpha$ 1); Gal3, galectin 3; Gastroc, gastrocnemius; *Tnfa*, tumor necrosis factor- $\alpha$ .



dystroglycan (*Dag1*),  $\alpha$  sarcoglycan (*Sgca*), and laminin  $\alpha 2$  (*Lama2*), showed no increases in any group relative to control (data not shown). In aggregate, these gene expression studies suggest that *CMAH* transgene expression, either alone (group 2) or in the context of elevated Neu5Gc antibodies (group 1), can induce expression of markers of muscle inflammation in *Cmah*<sup>-/-</sup>*mdx* mice.

## Discussion

Modeling the human *CMAH* gene inactivating deletion in *Cmah*<sup>-/-</sup> mice has led to numerous insights into how changes in the human sialoglycome may have altered human biological function. Mice lacking *Cmah* have impaired wound healing, impaired hearing, an increased propensity to diabetes, a changed gut microbiome and responses to bacterial challenge, altered responses to tumor cell metastasis, and increased inflammatory responses, which in the case of lipopolysaccharide challenge can cause increased death.<sup>17–21</sup> These same increased inflammatory responses are largely found when *Cmah* mice are crossed into mouse models for muscular dystrophy (*mdx* and *Sgca*<sup>-/-</sup>).<sup>8,26</sup> Another subsequent study has shown changed cardiac function.<sup>37</sup>

Herein, it was found that the increased disease severity of *Cmah*<sup>-/-</sup>*mdx* correlated with the presence of anti-Neu5Gc immunity and Neu5Gc expression in muscle. In the absence of Neu5Gc immunity, more muted phenotypic changes were found in *Cmah*<sup>-/-</sup>*mdx* mice relative to their *mdx* counterparts, but the severity of these phenotyping changes could be increased by adding back anti-Neu5Gc immunity through immunization with Neu5Gc-rich chimpanzee red blood cell ghosts, coupled with inducing *CMAH* transgene overexpression to produce large amounts of Neu5Gc. Anti-Neu5Gc antibodies could also be induced, albeit at lower levels, by systemic *CMAH* transgene expression in *Cmah*<sup>-/-</sup>*mdx* mice in the absence of immunization with Neu5Gc, which also impacted disease, particularly in the heart. Mice immunized with a Neu5Gc-rich immunogen, in combination with muscle *CMAH* transgene expression, showed significant decreases in survival and increases in skeletal muscle wasting and cardiac fibrosis.

These studies suggest that such dietary loading of sialic acid into skeletal muscle in *Cmah*<sup>-/-</sup>*mdx* mice, at least using a glycoprotein source for the Neu5Gc glycan, does not occur to an appreciable degree. Although it is still not clear how to account for the varied Neu5Gc expression that may occur in *Cmah*<sup>-/-</sup>*mdx* muscles, sialic acid, as a monosaccharide, can be loaded into skeletal muscle from diet when given in high amounts.<sup>55</sup> Thus, sialic acid expression in *Cmah*-deficient muscles, including human muscles, may vary depending on diet in ways that are not easily controlled for. Dietary glycoprotein would be the predominant source of Neu5Gc in a normal human diet, although the presence of

Neu5Gc in other tissues, where Neu5Gc is known to be more readily loaded from diet,<sup>10</sup> may also contribute to muscle disease in ways not yet explored. Although these experiments were generally unsuccessful in inducing Neu5Gc autoimmunity in *Cmah*<sup>-/-</sup>*mdx* mice using only dietary Neu5Gc loading from a glycoprotein source, humans clearly show a more robust induction of dietary-based Neu5Gc autoimmunity, which may be triggered by the scavenging and presentation of dietary Neu5Gc on lipooligosaccharides of human-specific commensal pathogens, such as nontypeable *Hemophilus influenzae*.<sup>13</sup> The mouse digestive system microbiome may also possess bacteria that can present dietary Neu5Gc to induce Neu5Gc autoimmunity, but these microbes have not yet been defined.

Inducing anti-Neu5Gc immunity in *Cmah*<sup>-/-</sup>*mdx* mice is important for modeling DMD human disease not only because it can impact disease severity but because anti-Neu5Gc antibodies can be present in DMD patients. These experiments have shown that anti-Neu5Gc antibodies are present at increased levels in some, but not all, DMD patients relative to age-matched otherwise normal subjects, and that such antibodies recognized Neu5Gc in the context of a large number of different subterminal glycan structures. As Neu5Gc expression is detectable in DMD skeletal muscle,<sup>51</sup> such anti-Neu5Gc antibodies could target Neu5Gc present in muscle to increase disease pathogenesis, exacerbating muscle inflammation. Thus, xenosialitis caused by Neu5Gc may help amplify muscle inflammation that is already present in DMD, which in turn may drive further Neu5Gc uptake in muscle, generating a vicious cycle. Neither of these mechanisms are expected to be present in the absence of muscle disease (eg, in healthy human or *Cmah*<sup>-/-</sup> muscle). Furthermore, as anti-Neu5Gc antibodies against many Neu5Gc-containing glycans showed significant reductions with age in DMD patients, the contribution of xenosialitis to disease might be greater in younger patients, in whom more muscle mass is present. Given that dietary intake of Neu5Gc appears to be sufficient to induce Neu5Gc autoimmunity in humans, and can begin shortly after weaning,<sup>13</sup> such results raise the possibility that eliminating dietary Neu5Gc (eg, red meat) may ameliorate DMD disease pathology and progression.

## Acknowledgments

We thank Kevin Flanigan (Nationwide Children's Hospital) for assistance with analysis of Duchenne muscular dystrophy and normal human serum samples; and Genevieve Faber for technical support.

## Author Contributions

P.T.M., K.K., and A.V. wrote the manuscript with editorial input from other authors. B.G., A.M., D.Z., A.A., K.E.C., and P.T.M performed all biochemical, cell biology,



molecular biology, and pathology studies on mice. K.K., S.D., A.S., B.G., K.E.C., P.T.M., and A.V. analyzed immune titers. P.M.L.J. performed muscle physiology studies and J.O., S.D., and A.V. performed high-performance liquid chromatography studies.

## Supplemental Data

Supplemental material for this article can be found at <http://doi.org/10.1016/j.ajpath.2021.04.015>.

## References

- Varki A: Multiple changes in sialic acid biology during human evolution. *Glycoconj J* 2009, 26:231–245
- Schwarzkopf M, Knobloch KP, Rohde E, Hinderlich S, Wiechens N, Lucka L, Horak I, Reutter W, Horstkorte R: Sialylation is essential for early development in mice. *Proc Natl Acad Sci U S A* 2002, 99: 5267–5270
- Varki A: Colloquium paper: uniquely human evolution of sialic acid genetics and biology. *Proc Natl Acad Sci U S A* 2010, 107 Suppl 2: 8939–8946
- Shaw L, Schneckenburger P, Carlsen J, Christiansen K, Schauer R: Mouse liver cytidine-5'-monophosphate-N-acetylneuraminic acid hydroxylase: catalytic function and regulation. *Eur J Biochem* 1992, 206: 269–277
- Kawano T, Koyama S, Takematsu H, Kozutsumi Y, Kawasaki H, Kawashima S, Kawasaki T, Suzuki A: Molecular cloning of cytidine monophospho-N-acetylneuraminic acid hydroxylase: regulation of species- and tissue-specific expression of N-glycolylneuraminic acid. *J Biol Chem* 1995, 270:16458–16463
- Chou HH, Takematsu H, Diaz S, Iber J, Nickerson E, Wright KL, Muchmore EA, Nelson DL, Warren ST, Varki A: A mutation in human CMP-sialic acid hydroxylase occurred after the Homo-Pan divergence. *Proc Natl Acad Sci U S A* 1998, 95: 11751–11756
- Okerblom J, Fletes W, Patel HH, Schenk S, Varki A, Breen EC: Human-like *Cmah* inactivation in mice increases running endurance and decreases muscle fatigability: implications for human evolution. *Proc Biol Sci* 2018, 285:20181656
- Chandrasekharan K, Yoon JH, Xu Y, deVries S, Camboni M, Janssen PM, Varki A, Martin PT: A human-specific deletion in mouse *Cmah* increases disease severity in the mdx model of Duchenne muscular dystrophy. *Sci Transl Med* 2010, 2:42ra54
- Oetke C, Hinderlich S, Brossmer R, Reutter W, Pawlita M, Keppler OT: Evidence for efficient uptake and incorporation of sialic acid by eukaryotic cells. *Eur J Biochem* 2001, 268: 4553–4561
- Banda K, Gregg CJ, Chow R, Varki NM, Varki A: Metabolism of vertebrate amino sugars with N-glycolyl groups: mechanisms underlying gastrointestinal incorporation of the non-human sialic acid xeno-autoantigen N-glycolylneuraminic acid. *J Biol Chem* 2012, 287: 28852–28864
- Tangvoranuntakul P, Gagneux P, Diaz S, Bardor M, Varki N, Varki A, Muchmore E: Human uptake and incorporation of an immunogenic nonhuman dietary sialic acid. *Proc Natl Acad Sci U S A* 2003, 100:12045–12050
- Bardor M, Nguyen DH, Diaz S, Varki A: Mechanism of uptake and incorporation of the non-human sialic acid N-glycolylneuraminic acid into human cells. *J Biol Chem* 2005, 280:4228–4237
- Taylor RE, Gregg CJ, Padler-Karavani V, Ghaderi D, Yu H, Huang S, Sorensen RU, Chen X, Inostroza J, Nizet V, Varki A: Novel mechanism for the generation of human xeno-autoantibodies against the nonhuman sialic acid N-glycolylneuraminic acid. *J Exp Med* 2010, 207:1637–1646
- Diaz SL, Padler-Karavani V, Ghaderi D, Hurtado-Ziola N, Yu H, Chen X, Brinkman-Van der Linden EC, Varki A, Varki NM: Sensitive and specific detection of the non-human sialic acid N-glycolylneuraminic acid in human tissues and biotherapeutic products. *PLoS One* 2009, 4:e4241
- Nguyen DH, Tangvoranuntakul P, Varki A: Effects of natural human antibodies against a nonhuman sialic acid that metabolically incorporates into activated and malignant immune cells. *J Immunol* 2005, 175:228–236
- Padler-Karavani V, Yu H, Cao H, Chokhawala H, Karp F, Varki N, Chen X, Varki A: Diversity in specificity, abundance, and composition of anti-Neu5Gc antibodies in normal humans: potential implications for disease. *Glycobiology* 2008, 18:818–830
- Hedlund M, Padler-Karavani V, Varki NM, Varki A: Evidence for a human-specific mechanism for diet and antibody-mediated inflammation in carcinoma progression. *Proc Natl Acad Sci U S A* 2008, 105:18936–18941
- Byres E, Paton AW, Paton JC, Lofling JC, Smith DF, Wilce MC, Talbot UM, Chong DC, Yu H, Huang S, Chen X, Varki NM, Varki A, Rossjohn J, Beddoe T: Incorporation of a non-human glycan mediates human susceptibility to a bacterial toxin. *Nature* 2008, 456: 648–652
- Okerblom JJ, Schwarz F, Olson J, Fletes W, Ali SR, Martin PT, Glass CK, Nizet V, Varki A: Loss of CMAH during human evolution primed the monocyte-macrophage lineage toward a more inflammatory and phagocytic state. *J Immunol* 2017, 198:2366–2373
- Buchlis G, Odorizzi P, Soto PC, Pearce OM, Hui DJ, Jordan MS, Varki A, Wherry EJ, High KA: Enhanced T cell function in a mouse model of human glycosylation. *J Immunol* 2013, 191:228–237
- Hedlund M, Tangvoranuntakul P, Takematsu H, Long JM, Housley GD, Kozutsumi Y, Suzuki A, Wynshaw-Boris A, Ryan AF, Gallo RL, Varki N, Varki A: N-glycolylneuraminic acid deficiency in mice: implications for human biology and evolution. *Mol Cell Biol* 2007, 27:4340–4346
- Kwon DN, Park WJ, Choi YJ, Gurunathan S, Kim JH: Oxidative stress and ROS metabolism via down-regulation of sirtuin 3 expression in *Cmah*-null mice affect hearing loss. *Aging (Albany NY)* 2015, 7:579–594
- Kavaler S, Morinaga H, Jih A, Fan W, Hedlund M, Varki A, Kim JJ: Pancreatic beta-cell failure in obese mice with human-like CMP-Neu5Ac hydroxylase deficiency. *FASEB J* 2011, 25: 1887–1893
- Ghaderi D, Springer SA, Ma F, Cohen M, Secrest P, Taylor RE, Varki A, Gagneux P: Sexual selection by female immunity against paternal antigens can fix loss of function alleles. *Proc Natl Acad Sci U S A* 2011, 108:17743–17748
- Kwon DN, Chang BS, Kim JH: Gene expression and pathway analysis of effects of the CMAH deactivation on mouse lung, kidney and heart. *PLoS One* 2014, 9:e107559
- Martin PT, Camboni M, Xu R, Golden B, Chandrasekharan K, Wang CM, Varki A, Janssen PM: N-glycolylneuraminic acid deficiency worsens cardiac and skeletal muscle pathophysiology in alpha-sarcoglycan-deficient mice. *Glycobiology* 2013, 23:833–843
- Sicinski P, Geng Y, Ryder-Cook AS, Barnard EA, Darlison MG, Barnard PJ: The molecular basis of muscular dystrophy in the mdx mouse: a point mutation. *Science* 1989, 244:1578–1580
- Hoffman EP, Brown RH Jr, Kunkel LM: Dystrophin: the protein product of the Duchenne muscular dystrophy locus. *Cell* 1987, 51: 919–928
- Koenig M, Hoffman EP, Bertelson CJ, Monaco AP, Feener C, Kunkel LM: Complete cloning of the Duchenne muscular dystrophy (DMD) cDNA and preliminary genomic organization of the DMD gene in normal and affected individuals. *Cell* 1987, 50:509–517
- Deconinck AE, Rafael JA, Skinner JA, Brown SC, Potter AC, Metzinger L, Watt DJ, Dickson JG, Tinsley JM, Davies KE:

- Utrophin-dystrophin-deficient mice as a model for Duchenne muscular dystrophy. *Cell* 1997, 90:717–727
31. Grady RM, Teng H, Nichol MC, Cunningham JC, Wilkinson RS, Sanes JR: Skeletal and cardiac myopathies in mice lacking utrophin and dystrophin: a model for Duchenne muscular dystrophy. *Cell* 1997, 90:729–738
  32. Sacco A, Mourkioti F, Tran R, Choi J, Llewellyn M, Kraft P, Shkreli M, Delp S, Pomerantz JH, Artandi SE, Blau HM: Short telomeres and stem cell exhaustion model Duchenne muscular dystrophy in mdx/mTR mice. *Cell* 2010, 143:1059–1071
  33. Xu R, Singhal N, Serinagaoglu Y, Chandrasekharan K, Joshi M, Bauer JA, Janssen PM, Martin PT: Deletion of Galgt2 (B4Galnt2) reduces muscle growth in response to acute injury and increases muscle inflammation and pathology in dystrophin-deficient mice. *Am J Pathol* 2015, 185:2668–2684
  34. Rooney JE, Welsler JV, Dechert MA, Flintoff-Dye NL, Kaufman SJ, Burkin DJ: Severe muscular dystrophy in mice that lack dystrophin and alpha7 integrin. *J Cell Sci* 2006, 119:2185–2195
  35. Vo AH, McNally EM: Modifier genes and their effect on Duchenne muscular dystrophy. *Curr Opin Neurol* 2015, 28:528–534
  36. Ceco E, Bogdanovich S, Gardner B, Miller T, DeJesus A, JU Earley, Hadhazy M, Smith LR, Barton ER, Molkenin JD, McNally EM: Targeting latent TGFbeta release in muscular dystrophy. *Sci Transl Med* 2014, 6:259ra144
  37. Blain AM, Grealley E, McClorey G, Manzano R, Betts CA, Godfrey C, O'Donovan L, Coursindel T, Gait MJ, Wood MJ, MacGowan GA, Straub VW: Peptide-conjugated phosphodiesterase oligomer-mediated exon skipping has benefits for cardiac function in mdx and Cmah<sup>-/-</sup>mdx mouse models of Duchenne muscular dystrophy. *PLoS One* 2018, 13:e0198897
  38. Naito-Matsui Y, Davies LR, Takematsu H, Chou HH, Tangvoranuntakul P, Carlin AF, Verhagen A, Heyser CJ, Yoo SW, Choudhury B, Paton JC, Paton AW, Varki NM, Schnaar RL, Varki A: Physiological exploration of the long term evolutionary selection against expression of N-glycolylneuraminic acid in the brain. *J Biol Chem* 2017, 292:2557–2570
  39. Mahajan VS, Demissie E, Mattoo H, Viswanadham V, Varki A, Morris R, Pillai S: Striking immune phenotypes in gene-targeted mice are driven by a copy-number variant originating from a commercially available C57BL/6 strain. *Cell Rep* 2016, 15:1901–1909
  40. Landini G, Martinelli G, Piccinini F: Colour deconvolution - stain unmixing in histological imaging. *Bioinformatics* 2021, 37:1485–1487
  41. Ruifrok AC, Johnston DA: Quantification of histochemical staining by color deconvolution. *Anal Quant Cytol Histol* 2001, 23:291–299
  42. Samraj AN, Bertrand KA, Luben R, Khedri Z, Yu H, Nguyen D, Gregg CJ, Diaz SL, Sawyer S, Chen X, Eliassen H, Padler-Karavani V, Wu K, Khaw KT, Willett W, Varki A: Polyclonal human antibodies against glycans bearing red meat-derived non-human sialic acid N-glycolylneuraminic acid are stable, reproducible, complex and vary between individuals: total antibody levels are associated with colorectal cancer risk. *PLoS One* 2018, 13:e0197464
  43. Manzi AE, Diaz S, Varki A: High-pressure liquid chromatography of sialic acids on a pellicular resin anion-exchange column with pulsed amperometric detection: a comparison with six other systems. *Anal Biochem* 1990, 188:20–32
  44. Martin PT, Xu R, Rodino-Klapac LR, Oglesbay E, Camboni M, Montgomery CL, Shontz K, Chicoine LG, Clark KR, Sahenk Z, Mendell JR, Janssen PM: Overexpression of Galgt2 in skeletal muscle prevents injury resulting from eccentric contractions in both mdx and wild-type mice. *Am J Physiol Cell Physiol* 2009, 296: C476–C488
  45. Xu R, Jia Y, Zygmunt DA, Martin PT: rAAVrh74.MCK.GALGT2 protects against loss of hemodynamic function in the aging mdx mouse heart. *Mol Ther* 2019, 27:636–649
  46. Acharyya S, Villalta SA, Bakkar N, Bupha-Intr T, Janssen PM, Carathers M, Li ZW, Beg AA, Ghosh S, Sahenk Z, Weinstein M, Gardner KL, Rafael-Fortney JA, Karin M, Tidball JG, Baldwin AS, Guttridge DC: Interplay of IKK/NF-kappaB signaling in macrophages and myofibers promotes muscle degeneration in Duchenne muscular dystrophy. *J Clin Invest* 2007, 117:889–901
  47. Xiao X, Li J, Samulski RJ: Production of high-titer recombinant adeno-associated virus vectors in the absence of helper adenovirus. *J Virol* 1998, 72:2224–2232
  48. Zolotukhin S, Byrne BJ, Mason E, Zolotukhin I, Potter M, Chesnut K, Summerford C, Samulski RJ, Muzyczka N: Recombinant adeno-associated virus purification using novel methods improves infectious titer and yield. *Gene Ther* 1999, 6: 973–985
  49. Padler-Karavani V, Hurtado-Ziola N, Pu M, Yu H, Huang S, Muthana S, Chokhawala HA, Cao H, Secrest P, Friedmann-Morvinski D, Singer O, Ghaderi D, Verma IM, Liu YT, Messer K, Chen X, Varki A, Schwab R: Human xenautoantibodies against a non-human sialic acid serve as novel serum biomarkers and immunotherapeutics in cancer. *Cancer Res* 2011, 71:3352–3363
  50. Livak KJ, Schmittgen TD: Analysis of relative gene expression data using real-time quantitative PCR and the 2<sup>-</sup>(Delta Delta C(T)) method. *Methods* 2001, 25:402–408
  51. Martin PT, Golden B, Okerblom J, Camboni M, Chandrasekharan K, Xu R, Varki A, Flanigan KM, Kornejag JJ: A comparative study of N-glycolylneuraminic acid (Neu5Gc) and cytotoxic T cell (CT) carbohydrate expression in normal and dystrophin-deficient dog and human skeletal muscle. *PLoS One* 2014, 9:e88226
  52. Hoyte K, Kang C, Martin PT: Definition of pre- and postsynaptic forms of the CT carbohydrate antigen at the neuromuscular junction: ubiquitous expression of the CT antigens and the CT GalNAc transferase in mouse tissues. *Brain Res Mol Brain Res* 2002, 109: 146–160
  53. Kim ML, Chandrasekharan K, Glass M, Shi S, Stahl MC, Kaspar B, Stanley P, Martin PT: O-fucosylation of muscle agrin determines its ability to cluster acetylcholine receptors. *Mol Cell Neurosci* 2008, 39: 452–464
  54. Xu R, Jia Y, Zygmunt DA, Cramer ML, Crowe KE, Shao G, Maki AE, Guggenheim HN, Hood BC, Griffin DA, Peterson E, Bolon B, Cheatham JP, Cheatham SL, Flanigan KM, Rodino-Klapac LR, Chicoine LG, Martin PT: An isolated limb infusion method allows for broad distribution of rAAVrh74.MCK.GALGT2 to leg skeletal muscles in the rhesus macaque. *Mol Ther Methods Clin Dev* 2018, 10:89–104
  55. Malicdan MC, Noguchi S, Nishino I: A preclinical trial of sialic acid metabolites on distal myopathy with rimmed vacuoles/hereditary inclusion body myopathy, a sugar-deficient myopathy: a review. *Ther Adv Neurol Disord* 2010, 3:127–135